

The Effect of Fluorescence Lifetime and Energy Level in Small Molecules for Efficient Hybrid Solar Cells

Shuqiang Liu¹, Yu Xie^{1,*}, Xue Li², Yuancheng Qin^{1,*}, Mingjun Li¹, Jinsheng Zhao^{2,*}

¹Key Laboratory of Jiangxi Province for Persistent Pollutants Control and Resources Recycle, Nanchang Hangkong University, Nanchang, 330063, P. R. China;

²College of Chemistry and Chemical Engineering, Liaocheng University, Liaocheng, 252059, P.R. China.

*E-mail: xieyu_121@163.com, qinyuancheng@hotmail.com, j.s.zhao@163.com

Received: 28 October 2018 / Accepted: 24 January 2019 / Published: 7 February 2019

Two properties make organic semiconductor a good candidate for potential solar cell application: narrow band gap and long photoluminescence lifetime. The former benefit large short circuit current and high open circuit voltage while latter helps to achieve the separation of the photo-excited exciton in limited time. It is disappointing that the fluorescence lifetime of the photosensitizer is rarely studied, although a lot of efforts have been devoted to study the solar absorption and energy levels of the dyes. Herein we designed and synthesized three D- π -A type small molecules, **D-TPA**, **R-TPA** and **C-TPA**, using triphenylamine (**TPA**) unit as donor unit, thiophene as π -conjugation bridges, alkyl cyanoacetate, dicyanovinyl or rhodanine as acceptor units. By selecting the proper acceptor unit, **D-TPA** shows a narrower band gap and longer fluorescence lifetime than other dyes, and also resulting in an improvement of PCE, which enhances by 9.4% and 23.2% when compared to the **R-TPA** and **C-TPA**, respectively.

Keywords: Hybrid Solar Cells; Small Molecules; Fluorescence Lifetime; Energy Level; Acceptor

1. INTRODUCTION

Polymers and small molecules are the two typical kinds of electron donor materials in the Organic photovoltaic (OPV) device. Although the reported polymer solar cells demonstrate higher PCEs[1-4], it is found that for a given polymer structure, the processing properties and performances greatly depend on the batch-to-batch variations in solubility, molecular weight, polydispersity and purity[5,6]. In contrast, small molecules-based OPV devices exhibit prominent advantages in many ways. Firstly, the performance changes little with batch to batch variation, due to their consistent and clear molecular structures [7]. At present, the efficiency of small molecules for organic solar cells (SCs) has exceeded

7%, which is largely approach to the excellent performances of the polymer SCs [8,9].

Nowadays, a lot of attention has been put on organic-inorganic hybrid solar cells (HSCs) possessing advantages from both sides [10-15]. Nevertheless, there are few studies on HSCs applying small-molecule and inorganic semiconductors up to date. However, those HSCs using small molecule can hardly exceed an efficiency of 1% [16-18]. In order to enhance efficiencies even further, our target is to synthesize new small-molecule with long fluorescence lifetime and better aligned energy levels.

As can be expected, the photovoltaic performances of HSCs could be optimized by designing proper dye molecules with distinguished properties, such as excellent film formation ability, wider and more efficient absorption, better matched energy levels between the donor/acceptor and higher charge mobility, as well as better solubility[7]. Excellent sensitizer in the HSCs can not only harvest photons, but also maintain a long lifetime ensuring successful separation from photo-excited exciton within a limited time at the contact surface of the organic/inorganic interface [19]. To our disappointment, the highly excited state lifetime is too short to achieve effective separation in most existing organic semiconductors, thus leading to poor performance of the HSCs.

An ideal small molecule (sensitizer) should have a narrow band gap and a long exciton lifetime for the construction of photovoltaic device [11]. Many highly efficient small molecular SCs have employed the D- π -A type linear conjugated structures with the extended conjugation length, which can efficiently intensify and broaden the absorption spectra of the sensitizer. The D- π -A is a typical push-pull structural molecular configuration, consisting of a central building blocks (electron-donating unit (D)), end groups (electron-accepting unit (A)) and π -conjugation bridge (usually thiophene) [20]. Therefore, this kind of small molecule can effectively regulate and control band gap by altering central building blocks, end groups and the length of thiophene bridges. In fact, small molecules showed impressive performance in small molecule OPV [21,22]. Upon photoexcitation, electron transfer from the donor to the acceptor is a fast process to generate charge-separated species. In this respect, triphenylamine or substituted derivatives have been successfully used as donors for sensitizers in dye-sensitized solar cells. It has also been observed that the structure of the π -conjugated bridging group played a decisive role in device performance. The bridging group can serve both, as a part of the light absorbing chromophore and as a pathway for transporting charges.

Because of its good electron-donating and hole-transporting abilities [23], organic optoelectronic materials derived from triphenylamine (TPA) derivatives is one of the most excellent efficient photovoltaic materials, and have been widely investigated in terms of their photovoltaic performance. Besides, benefiting from special propeller starburst structure, materials could exhibit isotropic optical and charge-transporting properties when TPA combines with the systems of π -conjugated units. Small molecules based on TPA show the potential for high-efficiency photovoltaic applications [24-26]. Dicyanovinyl [27,28], alkyl cyanoacetate and rhodanine are introduced into D-A small molecules as electron acceptor for their capability of effectively exciting intramolecular charge transfer and lowering band gaps[29,30,21]. Besides, these acceptors have a simple conjugated structure and strong electron-withdrawing ability. The introduction of these molecules adjust the energy levels of the highest occupied molecular orbital (HOMO) and lowest unoccupied molecular orbital (LUMO) and improve the solubility.

As for the inorganic part in the HSCs, the TiO₂ is selected as the acceptor of the active layer for

its good electrical conductivity, and the TiO₂:P3HT-based solid-state solar cells have displayed excellent optical performance after inserting the TT1 dye layer, which could make the TiO₂ surface and P3HT separated properly, thus preventing the direct contact and thereby suppressing the charge recombination between them [31]. But take the stability of solar into consideration, the SCs with TiO₂ cannot stabilize in the inert atmosphere [32,33].

In this work, three kinds of D- π -A small molecules, **C-TPA**, **D-TPA**, and **R-TPA** Fig. 1 (a) were devised and synthesized. Among the small molecules, the **TPA** unit acts as central donor unit, thiophene as π -conjugation bridges. Dicyanovinyl (**D**), alkyl cyanoacetate (**C**) or rhodanine (**R**) play the role of acceptor unit. Herein, much attention was put on the effects of electron-accepting unit on the fluorescence lifetime, energy level and the performance of the device. The schematic diagram was shown in Fig. 1 (b). This is different from the previous studies that mainly emphasized the importance on solar absorption and energy levels. By optimizing different acceptor, small molecule with a relatively long fluorescence lifetime is obtained. And the relationships among the acceptor units, fluorescence lifetimes, as well as the photovoltaic performance of the HSCs have been discussed in details. And the result of the present study may contribute to the design of the sensitizer materials used in HSCs.

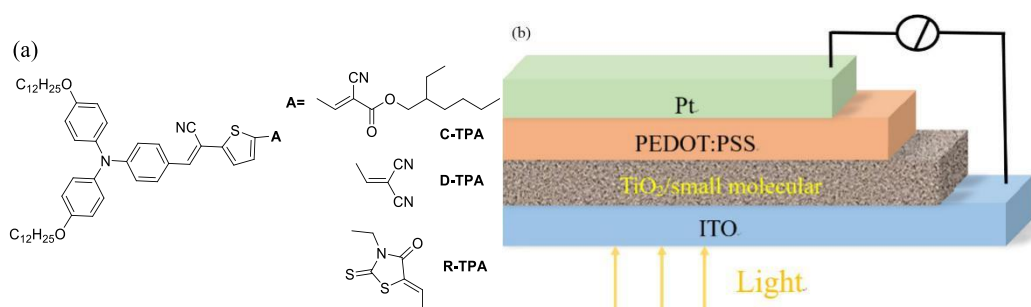


Figure 1. a) Chemical structure of **C-TPA**, **D-TPA**, and **R-TPA**. b) Schematic diagram of organic solar cells

2. EXPERIMENTAL

2.1. Materials and instruments

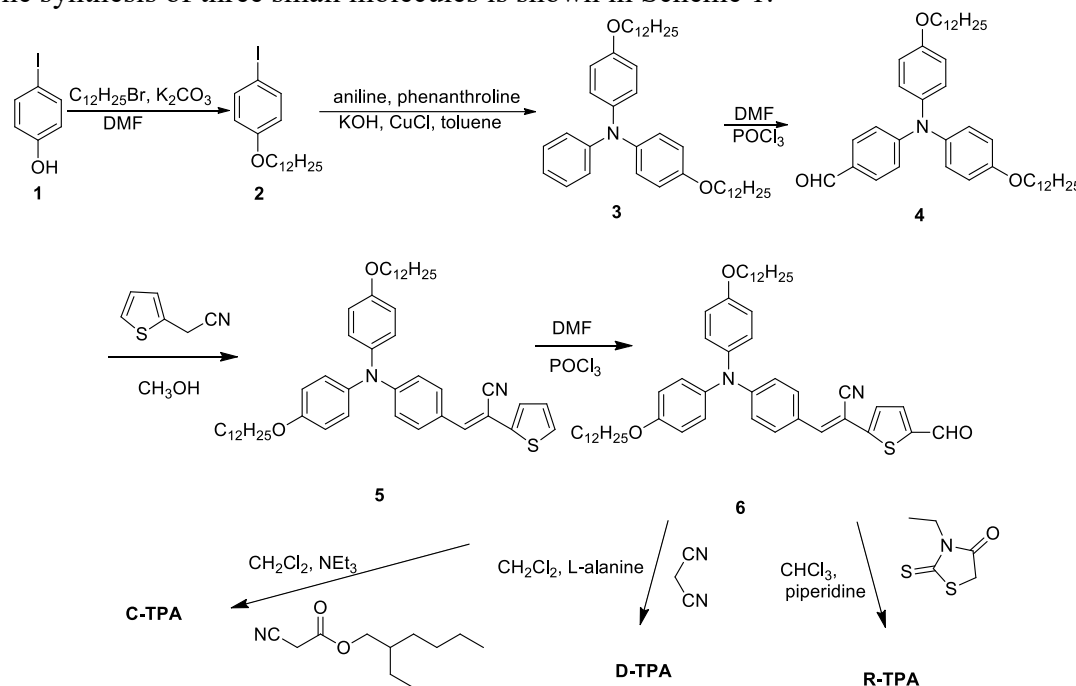
All materials are either commercially available or easily prepared and used without purification if not necessary. The solvent is dried when there is a requirement in the use of the reaction. Compound **4** (Scheme 1) (4-(bis(4-(dodecyloxy)phenyl)amino)benzaldehyde) was synthesized from the literature[34].

¹H and ¹³C NMR were used to confirm structure information of compounds, and was measured by a Bruker ARX 400 NMR spectrometer. Thermal stability analysis was carried out on a TGA Q600. UV-vis was recorded by a Perkin Elmer Lambda 900 UV-vis/NIR spectrometer. The cyclic voltammetry (CV) was carried out by A BAS 100B instrument, tetrabutylammonium hexafluorophosphate (TBAPF₆, 0.1 mol/L) was used as the electrolyte solution, a polished platinum disk electrode (surface area, 0.5 cm²) act as the working electrodes and an Ag/AgCl (Saturated potassium chloride solution) act as the

reference electrode. A platinum wire with a diameter of 1 mm was used as the counter electrode. Time resolved photo-luminescence measurements were performed on a spectrometer (Bruker Optics 250IS/SM). Femtosecond laser pulse was applied to motivate the samples, operating at 10 Hz and the final time resolution was determined to be ~ 10 ps. The power conversion efficiency (PCE) of HSCs were carried out on Xe Lamp Oriel Sol3A™ Class AAA Solar Simulators (94023A, USA) under a simulated sunlight from a 100 W xenon arc lamp in atmospheric environment.

2.2. Synthesis.

The synthesis of three small molecules is shown in Scheme 1.



Scheme 1. Synthetic routes to **C-TPA**, **D-TPA**, and **R-TPA**

2.2.1 The synthesis of (E)-3-(4-(bis(4-(dodecylphenoxy)phenyl)amino)phenyl)-2-(thiophen-2-yl)acrylonitrile (Compound 5)

1.3259 g of compound **4** (2mmol), 0.5 g of potassium tert-butoxide (7.8mmol) and 0.37 g of 2-thiophene acetonitrile (3mmol) were dissolved in 30 mL of methanol in a 50 mL single neck flask. Heat the mixture from room temperature to 60°C , and then be refluxed for 12 h. After which, the mixture was cooled down to room temperature, which was rinsed with distilled water and be extracted with CH_2Cl_2 for several times. The organic layer was collected and then be dried with anhydrous MgSO_4 and then was concentrated by a vacuum rotatory evaporator. The crude product was purified by column chromatography (eluant: dichloromethane : n-hexane= 3:2) to give compound **5** as 0.37 g, a yellow-green solid (1.29 g, yield: 85.5%). ^1H NMR (CDCl_3 , 400MHz, δ/ppm): 7.65(d, 2H), 7.25(d, 1H), 7.18(t, 1H), 7.07(d, 1H), 6.99(t, 4H), 6.98(s, 1H), 6.85(t, 6H), 3.92(t, 4H), 1.76(m, 4H), 1.44(d, 4H), 1.26(s,

32H), 0.87(t, 6H). ^{13}C NMR (CDCl_3 , 100MHz, /ppm): 156.4, 130.5, 127.5, 117.9, 115.4, 31.9, 29.4, 22.6, 14.1.

2.2.2 (*E*)-3-(4-(bis(4-(dodecyloxy)phenyl)amino)phenyl)-2-(5-formylthiophen-2-yl) acrylonitrile (compound 6)

POCl_3 (3.5 mL) and N, N-dimethylformamide (6 mL) were put into a 25 mL three-neck flask under argon atmosphere at 0 °C and be stirred for 1h. 1.18 g of compound **5** (1.58 mmol) was dissolved in 1.5 mL of 1, 2-dichloroethane, and then the solution was added into the above-mentioned three-necked flask. The obtained mixture was stirred magnetically and refluxed overnight, and then cooled to 25°C. The crude product was rinsed with water and be extracted with CH_2Cl_2 for several times. The organic phase was collected and be dried over dry MgSO_4 , and be concentrated for the purification purpose. And the purification process was carried out by chromatographic column (eluant: dichloromethane: n-hexane = 4:1). Finally, compound **6** was obtained as red solid (1.02 g, yield: 77.6%). ^1H NMR (CDCl_3 , 400MHz, δ /ppm): 9.83 (s, 1H), 7.72 (d, 2H), 7.67 (d, 1H), 7.37 (m, 1H), 7.27 (s, 1H), 7.10 (d, 4H), 6.86 (t, 6H), 3.94 (t, 4H), 1.78 (t, 4H), 1.71 (s, 7H), 1.267 (s, 64H), 0.87 (d, 11H). ^{13}C NMR (CDCl_3 , 100MHz, δ /ppm): 182.3, 156.9, 127.8, 117.2, 115.5, 31.9, 29.6, 26.1, 22.7, 14.1.

2.2.3 The synthesis of C-TPA (Scheme 1)

Compound **6** (0.4376 g, 0.193 mmol), dry CH_2Cl_2 (28 mL), 2-ethylhexyl cyanoacetate (1.35 mL, 6.73mmol) and triethylamine were put into a 50 mL of single neck flask under argon. The solution was stirred overnight at 25 °C. The crude product was extracted with CH_2Cl_2 and rinsed with H_2O for three times. The organic phase was dried over anhydrous NaSO_4 . The solvent was removed by reduced pressure distillation, and the obtained residue was purified by column chromatography (eluant: dichloromethane: n-hexane = 2:3). Finally, **C-TPA** was collected as a light yellow solid (0.1324 g, 63.4 % yield). ^1H NMR (CDCl_3 , 400MHz, δ /ppm): 8.05 (s, 1H), 7.81 (d, 2H), 7.72 (m, 2H), 7.54 (m, 2H), 7.11 (d, 4H), 6.90 (d, 4H), 6.83(d, 2H), 5.35 (m, 6H), 4.39 (m, 4H), 4.23 (m, 4H), 2.23 (t, 1H), 2.03 (s, 2H), 2.01 (s, 1H), 1.87 (m, 4H) ^{13}C NMR (CDCl_3 , 100MHz, δ /ppm): 157.1, 128.0, 115.6, 53.4, 31.9, 29.6, 29.4, 22.7, 14.2. ESI HRMS: $[\text{M}^+]$ 954.30 calcd. for $\text{C}_{61}\text{H}_{83}\text{O}_4\text{N}_3\text{S}$ 954.36. Anal. calcd for $\text{C}_{61}\text{H}_{83}\text{O}_4\text{N}_3\text{S}$: C 76.70, H 8.80, N 4.39; found: C 76.76, H 8.77, N 4.40.

2.2.4 The synthesis of D-TPA

0.2 g of compound 6 (0.564 mmol), 5 mL of dry CH_2Cl_2 and malononitrile (25.7 mg, 0.389mmol) were put into a 25 mL single flask under argon. L-alanine (15 mg, 0.169 mmol) were dissolved in dry ethanol (4.5 mL) to get a solution and then was added to the flask. The mixture was heated to 40 °C, and then was stirred and refluxed for 12 h. Afterwards, the mixture was cooled down, which was then extracted with CH_2Cl_2 and be rinsed with H_2O for three times. The organic layer was dried over anhydrous NaSO_4 . The organic solvent of the above mixture was removed by vacuum

distillation under 0.1 vacuum degree, and then the residue was purified by column chromatography (eluant: dichloromethane : n-hexane = 1:2) to give **D-TPA** as a navy blue solid (0.134 g, yield: 58.7 %). ^1H NMR (CDCl_3 , 400MHz, δ/ppm): 7.77 (d, 2H), 7.75 (t, 2H), 7.61 (d, 1H), 7.53 (t, 2H), 7.41 (s, 1H), 7.35 (d, 1H), 7.12 (d, 3H), 6.89 (s, 2H), 6.87 (d, 2H), 6.84 (s, 1H), 4.20 (m, 2H), 3.95 (t, 2H), 1.77 (m, 3H), 1.70 (m, 2H), 1.43 (m, 8H), 1.31 (t, 16H), 1.28 (d, 25H). ^{13}C NMR (CDCl_3 , 100MHz, δ/ppm): 167.8, 157.1, 130.9, 128.8, 127.9, 115.6, 38.7, 29.6, 22.9, 14.1, 11.0. ESI HRMS: $[\text{M}^+]$ 823.10 calcd. for $\text{C}_{53}\text{H}_{66}\text{O}_2\text{N}_4\text{S}$ 823.15. Anal. calcd for $\text{C}_{53}\text{H}_{66}\text{O}_2\text{N}_4\text{S}$ C 76.28, H 8.11, N 6.79; found: C 77.32, H 8.08, N 6.81.

2.2.5 The synthesis of R-TPA

6 (0.258 mmol), 28 mL of dry chloroform and 3-ethyl-rhodanine (487.5 mg, 3 mmol) were added to a 50 mL of round-bottomed flask under argon. Piperidine (1 mmol) was added to the above mixture as the catalyst in the reaction. After heating to 110 °C, the mixture was stirred and refluxed for 12 h. After be cooled down, the resulting solution was extracted with CH_2Cl_2 and H_2O . The liquid phase of the next layer was collected, drying over anhydrous Na_2SO_4 . **R-TPA** was got by column chromatography (eluant: dichloromethane : n-hexane = 1:2) as purple red solid (0.166g, yield: 70.6 %). ^1H NMR (CDCl_3 , 400MHz, δ/ppm): 7.62 (s, 1H), 7.27 (d, 3H), 7.11 (d, 4H), 6.87 (d, 7H), 4.19 (t, 2H), 3.94 (t, 4H), 1.78 (t, 4H), 1.62 (s, 4H), 1.26 (s, 36H), 0.88(t, 6H). ^{13}C NMR (CDCl_3 , 100MHz, δ/ppm): 193.1, 156.8, 138.6, 132.5, 127.8, 115.5, 39.2, 31.9, 29.6, 26.1, 22.7, 14.0. ESI HRMS: $[\text{M}^+]$ 918.30 calcd. for $\text{C}_{55}\text{H}_{71}\text{O}_3\text{N}_3\text{S}_3$ 918.34. Anal. calcd for $\text{C}_{55}\text{H}_{71}\text{O}_3\text{N}_3\text{S}_3$: C 71.90, H 8.82, N 4.55; found: C 71.93, H 7.79, N 4.58.

2.3. Device fabrication

The device was fabricated with the general architecture: ITO/ TiO_2 /small molecular /PEDOT:PSS/Pt. All efficiency measurements are based on this structure. The TiO_2 was made by a similar way according to literature[35]. With n-type TiO_2 coated on Indium Tin Oxide (ITO) by spin-coating technique, a thickness 200~300nm of TiO_2 was prepared, and then the TiO_2 film was sintered in atmospheric environment at 400 °C for 25 min. After that, TiO_2 film were immersed into the dye solution (10 mg/mL in CHCl_3) overnight to let the p-type small molecular permeate into the TiO_2 layer, and then and the modified ITO electrode was dried under nitrogen atomosphere. The following is that the PEDOT:PSS as hole transport layer was spin coated onto the orgnic/inorganic hybrid layer on the ITO electrode. Lastly, with Pt electrodes are placed on the top by vacuum coating, the device was prepared successfully.

3. RESULTS AND DISCUSSION

3.1. Synthesis and Characterization

For all molecules, TPA work as donor unit while cyanoacetate (**C**) dicyanovinyl (**D**) or rhodanine

(**R**) unit as the acceptors. The detailed synthetic routes to **C-TPA**, **D-TPA**, and **R-TPA** are outlined in Scheme 1. The intermediate, 4-(bis(4-(dodecyloxy)phenyl)amino)benzaldehyde (**4**) was synthesized through a three-step reactions from 4-iodophenol (**1**) according to literature procedures[34]. The aldehydes (**4**) and thiophene-2-acetonitrile were condensed by Knoevenagel Condensation to give compound **5**, which underwent Vilsmeier reaction to yield compound **6**. Finally, the target small molecule **C-TPA** was obtained in good yield by the Knoevenagel condensation reaction with 2-ethylhexyl 2-cyanoacetate in the presence of catalytic amounts of triethylamine. **D-TPA** and **R-TPA** were synthesized by using the same reactions with malononitrile and 3-ethyl-2-thioxothiazolidin-4-one in the presence of L-alanine and piperidine, respectively. The structures of **C-TPA**, **D-TPA** and **R-TPA** were confirmed with NMR spectroscopy. **C-TPA**, **D-TPA** and **R-TPA** are soluble in common organic solutions. Thermogravimetric analysis (TGA) was used to investigate the thermal stability properties of **C-TPA**, **D-TPA**, and **R-TPA**. As shown in Fig. 2, **C-TPA**, **D-TPA** and **R-TPA** exhibit good thermal stability, with 5% mass loss temperature (T_d) at 226, 223 and 273°C under a nitrogen atmosphere, respectively. The thermal stability of **C-TPA**, **D-TPA**, and **R-TPA** is adequate for application in processed HSCs.

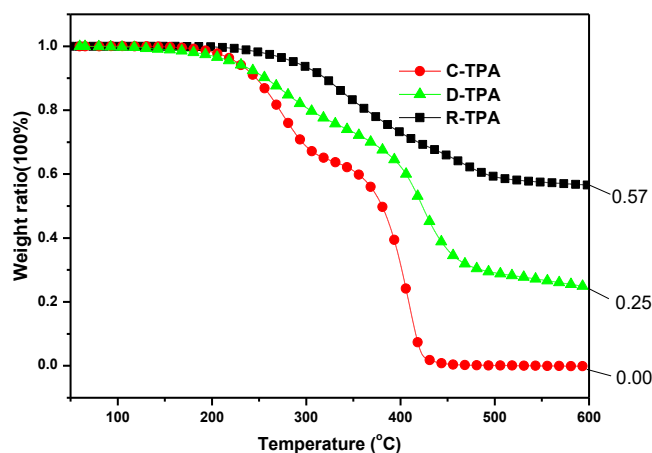


Figure 2. TGA thermograms of **C-TPA**, **D-TPA**, and **R-TPA**

3.2. Optical Properties

UV-Vis absorption of **C-TPA**, **D-TPA**, and **R-TPA** are summarized in Table 1. As shown in Fig. 3, the absorption peaks for **C-TPA**, **D-TPA**, and **R-TPA** are at 436, 561 and 483 nm, respectively. Three small molecules are absorbed at 350-700 nm, especially the **D-TPA** displays the nature of strong charge transport existing inside the molecules between the conjugated backbone of TPA and the acceptor. The absorption peaks of **D-TPA** revealed about 125 and 78 nm red shift compared with **C-TPA** and **R-TPA**, respectively. The optical band gap was calculated from band edges of the optical absorption spectra, which is 2.27 and 1.77 and 2.07 eV for **C-TPA**, **D-TPA**, and **R-TPA**, respectively, with **D-TPA** has the lowest bandgap among three molecules. By tailoring the acceptor structures, the optical band gap and absorption range was tuned, the three small molecules show wide absorption on whole visible wavelength range of the **TPA**-based small molecules, which indicate their potential application in HSCs.

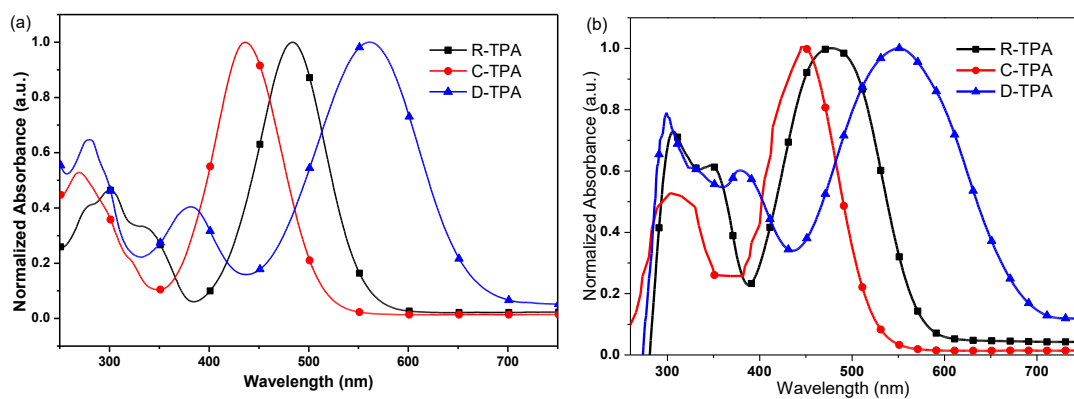


Figure 3. a) UV-Vis absorption spectra of C-TPA, D-TPA, R-TPA in chloroform and b) in film

Table 1. Optical, electrochemical and thermal stability data for C-TPA, D-TPA, and R-TPA

	$\lambda_{\max}(\text{nm})$	$E_{g, \text{opt}}(\text{eV})$	HOMO	LUMO	$E_{g, \text{cv}}(\text{eV})$	$T_d(^{\circ}\text{C})$
C-TPA	436	2.27	-5.35	-3.45	1.90	226
D-TPA	561	1.77	-5.38	-3.56	1.82	223
R-TPA	483	2.07	-5.40	-3.55	1.85	287

3.3. Electrochemical Characterization

The CV technique was used to investigate the electrochemical properties of C-TPA, D-TPA, and R-TPA. The test method has been described in our previous work[35]. The measured value of the CV of the small molecules modified thin films are shown in Fig. 4. The bandgap (E_g) based on the HOMO and LUMO values of C-TPA, D-TPA, and R-TPA were found to be about 1.90, 1.82 and 1.85 eV, respectively.

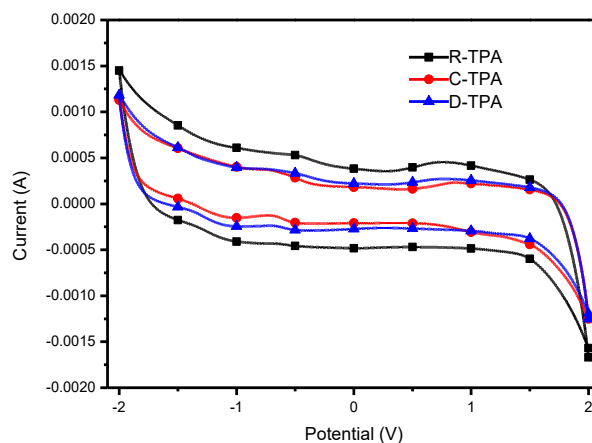


Figure 4. Cyclic voltammogram measurements of different small molecules

These data suggested that the introduction of different acceptor terminal units in these TPA

derivatives can tune effectively the electrochemical properties and optical band gaps of the resultant molecules. The D-TPA displays smaller electrochemical band gap and the optical band gap.

3.4. Theoretical Calculations.

In order to figure out the electronic structures of these small molecules, Density functional theory (DFT) calculations were conducted after majorizing the three dimensional geometric structures. Quantum mechanical calculations revealed that all small molecules have a similar zig-zag structure. These molecules are synthesized in a similar way, with TPA as a molecular skeleton and different acceptors applied which is hardly affecting main skeleton. However, because of the introduction of different units, which lead to the distribution of wave function in the molecular orbital to a certain extent and the changes of dihedral angle between the thiophene and the acceptors or the adjacent benzene plane. As can be seen from the **Fig.6**, the local electron density shows strong electronic driving force along the backbone, resulting from the difference of electron distribution between the TPA and acceptors. That can be good for the intramolecular charge transfer along the small molecule, thus extending the π -conjugation. The LUMO orbitals of these molecules are uniformly distributed on the electron acceptor groups and adjacent conjugated bridges, which is in favor of the charge separation and transfer in the excited state of the small molecules, indicating that the intramolecular charge transfer from aniline donor groups to acceptors take place effectively, while the HOMO orbitals are mainly distributed on the aniline donor groups[36,37]. In addition, in the occupied orbitals of the whole energy range, aparting from the radical chain outside, other atomic group had little contributions to the density of states, the delocalization distribution of HOMO is conducive to intramolecular charge carrier mobility, ensuring the photo-chemical activity of the molecule. As shown in Table 1, The HOMO of the three small molecules is relatively close. However, the energy band gap of **D-TPA** is the smallest, which is in accordance with the experimental data and the widest absorption spectrum.

In order to better understand the planarity of **D-TPA**, **R-TPA**, **C-TPA**, the dihedral angle between the thiophene and adjacent units are calculated through theoretical calculation. Theoretically speaking, improving the planarity of molecular is conducive to enhance the intramolecular π -electron delocalization, and improve the charge transfer ability[38]. Note that TPA is not a planar unit, for the reason that C-N bond employ the SP³ hybrid orbital approach. So we only focus on the dihedral angle between thiophene and adjacent benzene group or acceptor unit. It can be seen from Fig. 5, dihedral angles between the thiophene and acceptors unit for **D-TPA**, **R-TPA**, **C-TPA** are 2.3°, 0.4°, 1.1° respectively. Considering that the dihedral angles between the acceptor unit and the thiophene unit are small, the two units of the three molecules can be approximately considered to be on the same plane. The dihedral angles between the thiophene and the adjacent benzene appear difference, due to the attachment of different acceptor units of different electronegativities, the dihedral angle between the thiophene and benzene unit for **D-TPA**, **R-TPA**, **C-TPA** are 13°, 15°, 17° respectively. Overall speaking, **D-TPA** has better molecular planarity. Theoretically, **D-TPA** is stronger than the **R-TPA** and **C-TPA** in electron transport capability and intermolecular interaction, thus display better optical properties.

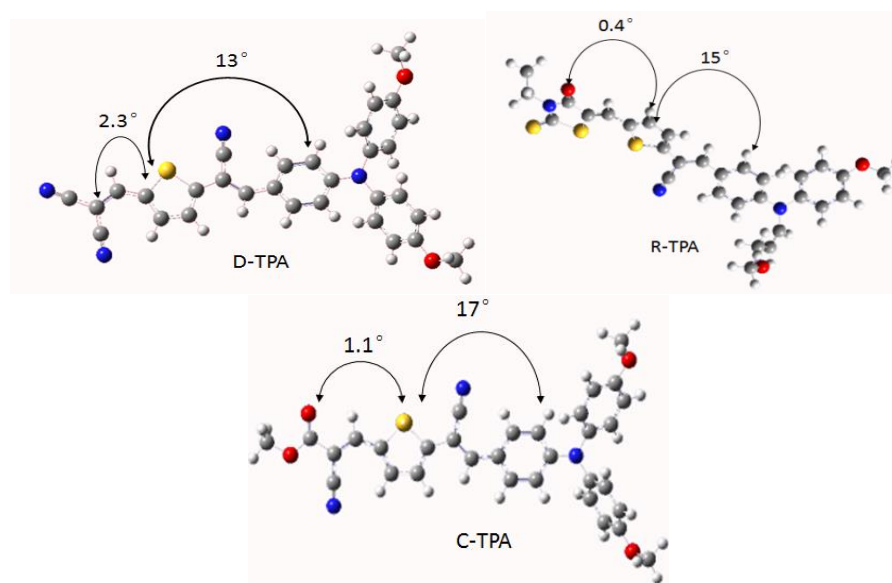


Figure 5. The dihedral angle between the thiophene and adjacent unit, obtained by the DFT/B3LYP/6-31G*method

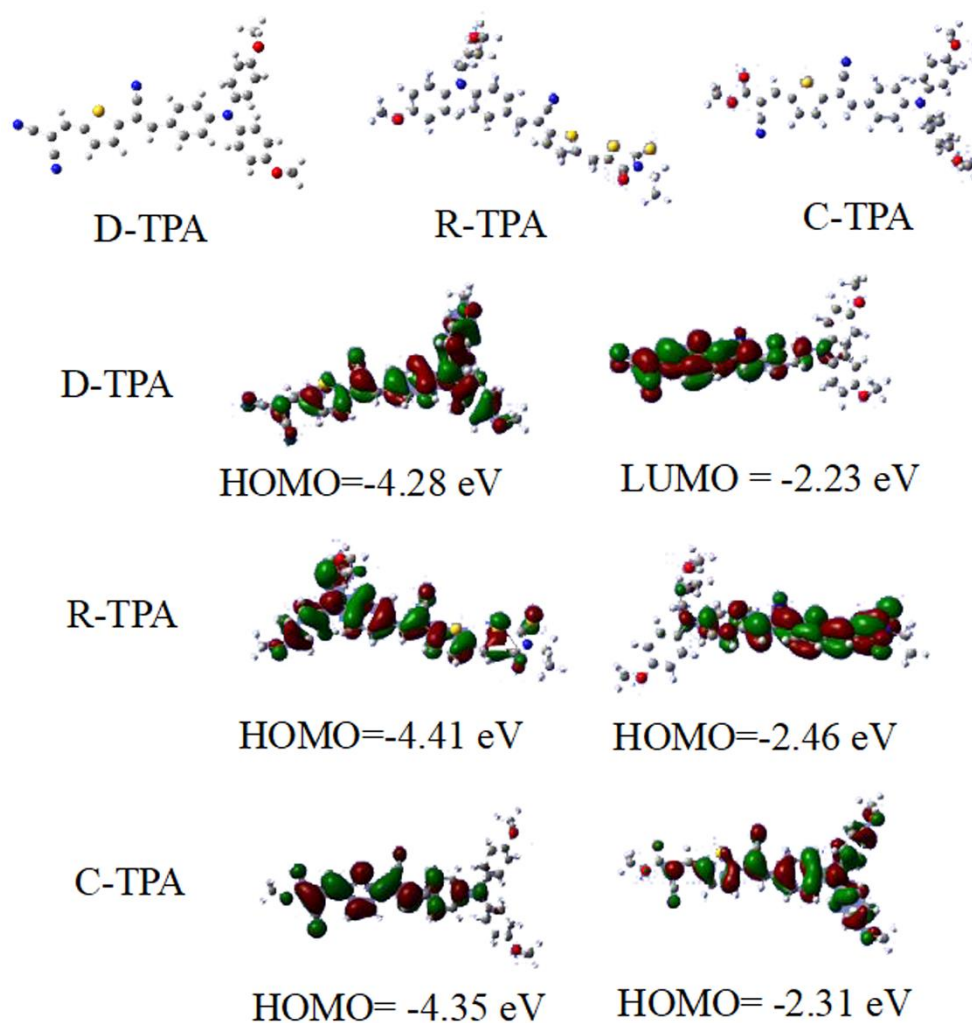


Figure 6. Optimized geometry and molecular orbital surfaces of the HOMO and LUMO of the model compounds, obtained by the DFT/B3LYP/6-31G* method.

3.5. Fluorescence lifetime of the small molecules

Herein we study the fluorescence lifetime of the three small molecules. The fluorescence lifetime is the average time that indicates the lifetime of the excited state. Relatively long lifetime is crucial for the exciton to get good separation in the interface between the TPA and acceptor units. Spectral signatures can be used to distinguish the excitons related to the process of intramolecular charge transfer (ICT). For the purpose to get their fluorescence lifetime, instant photo-luminescence experiment owning a time resolution of ~ 30 ps was applied. An appropriate pump wavelength (500 nm) have been chosen to excite the small molecular in the low-energy absorption band. Fig. 7 shows the fluorescence decays of the three small molecules. All of the small molecules show almost the same performance in negative delay time, resulting from the instant response of auto-correlation of laser pulse. But the three curves show the trend of exponential decay on the right of coordinate. The decay is one stage with the falling speed more and more slow. From the downward trend of the curve, Single exponential function is found to be fit with the curve [39].

$$S(t) = \int_{-\infty}^{+\infty} G(t - \tau) [\delta(\tau) + \exp(-\tau / \tau_t)] d\tau \quad (1)$$

where S represents the signal of time, G represents a function related to background-free laser pulse auto-correlation, τ represents the time. The fluorescence decay time can be achieved by following expression

$$\tau = \tau_t \quad (2)$$

These fluorescence decays are in conformity with single exponential equation and listed in Table 2.

Table 2. The fluorescence lifetime of three small molecules

Small molecular	D-TPA	R-TPA	C-TPA
δ/ps	85	73	64

All the small molecules are shown to have shorter emission decay on ps time. Each data was collected repeatedly to guarantee its accuracy. In the electronic part of the hybrid system of D- π -A type small molecules, the **D-TPA** shows relatively longer exciton lifetime, slightly higher than **R-TPA** and **C-TPA**. It indicates that the fluorescence lifetime can be adjusted by changing acceptor unit. By altering the electron deficient acceptors unit, the interactions between internal groups of small molecules are tuned, thus leading to changes of delocalization of the excited states and different fluorescence lifetimes.

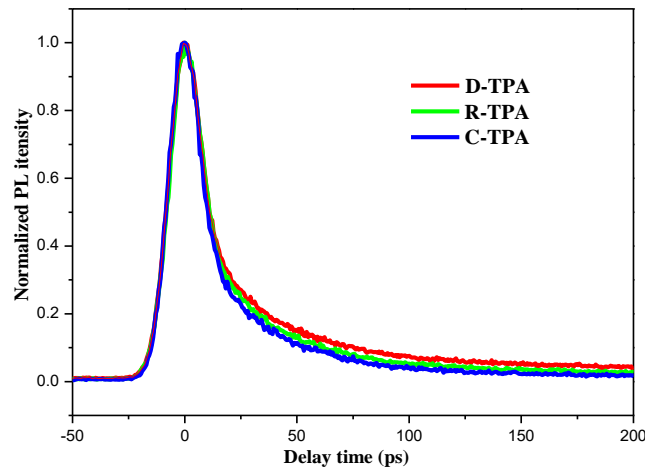


Figure 7. Time-resolved PL results of the small molecules

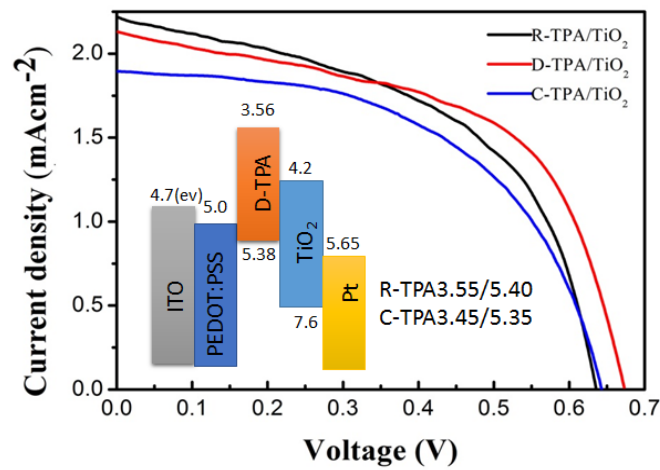


Figure 8. *J-V* characteristic curve of different small molecular OPVs. Inset: band structure of the OPVs

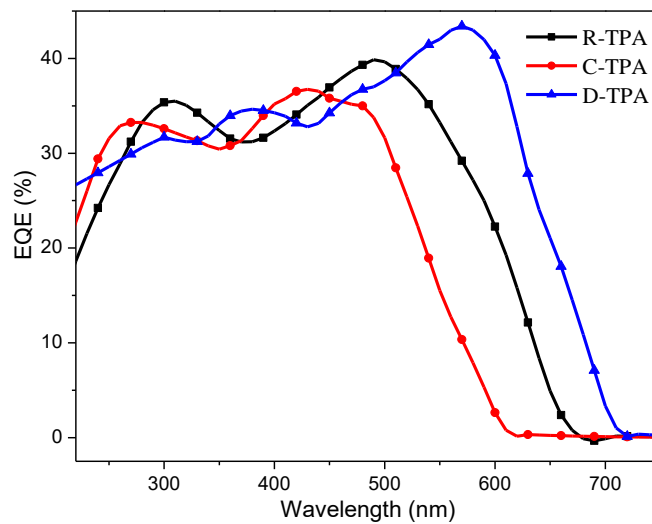


Figure 9. External quantum efficiency spectra of small molecules

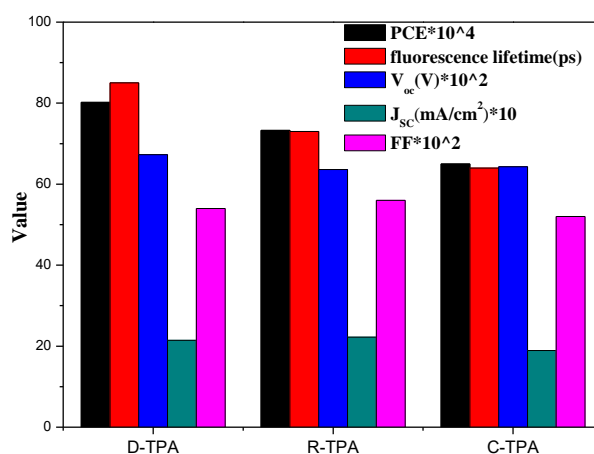
Table 3. The photovoltaic parameters of bulk hybrid solar cells

HSC	V_{oc} [V]	J_{sc}	FF	$^a\eta$ [%]
C-TPA/TiO₂	0.643 ± 0.13	1.895 ± 0.02	0.54 ± 0.01	0.649 ± 0.02
D-TPA/TiO₂	0.673 ± 0.11	2.146 ± 0.03	0.56 ± 0.03	0.800 ± 0.02
R-TPA/TiO₂	0.636 ± 0.10	2.221 ± 0.02	0.52 ± 0.01	0.730 ± 0.03

$$^a\eta = J_{sc} \cdot V_{oc} \cdot FF / P_{in}, P_{in} = 100 \text{ mW} \cdot \text{cm}^{-2} \text{ (AM 1.5)}$$

3.6. Photovoltaic Properties

For the purpose to make sense of the effect of different acceptors on the OPV efficiency, We have made characteristic battery device (ITO/PEDOT:PSS/small molecular/TiO₂/Pt) to explore their photovoltaic properties. J - V Characteristic curves of different small molecular are shown in **Fig.8** and summarized in Table 3. The C-TPA and R-TPA display a PCE of 0.649% and 0.734%, respectively. The **D-TPA** exhibits a relatively high efficiency of 0.802%, which is a little higher than the **C-TPA** and **R-TPA**. What is more, the external quantum efficiency (EQE) spectra of small molecules are shown in **Fig.9** and D-TPA displayed obviously higher absorption than that of R-TPA and C-TPA. We also find that the efficiency of the different small molecular increase with the decrease of the band gap. The narrower the band gap, the wider range of available light. That can be testified by the UV-Vis absorption spectra as shown in the **Fig. 3**. Summary of photovoltaic parameters can be seen in **Fig.10**.

**Figure 10.** Summary of photovoltaic parameters

Different acceptors units play an important role in adjusting energy levels, the acceptor units selected have different electron withdrawing ability. The deeper the HOMO energy level is, the higher open-circuit voltage is. Three kinds of small molecules in the HOMO-level gap is relatively small, so the open-circuit voltage of the three small molecules does not make much difference but the short-circuit current of **C-TPA** is small, caused by the large energy band-gap related to short-circuit current [40,41]. As to **D-TPA** and **R-TPA**, these two molecules have only a difference of 0.03 eV in band gap, so the

short circuit current of the two molecules does not make much difference. It seems to present a number of other factors, which determined the difference between the **C-TPA** and **D-TPA**. It is worth noting that **D** have two cyanos, it may be more advantageous to transfer electrons. However, it is difficult for us to find standard errors to correct error of the energy levels, and the energy levels can be finely tuned by other factors like the crystallinity and the electron withdrawing substituent position on small molecular. Therefore, accurate calculation of energy levels is not possible so far, although the dates can be reasonably explained.

4. CONCLUSIONS

To sum up, three D- π -A type small molecules, **C-TPA**, **D-TPA** and **R-TPA** have been devised and synthesized, which exhibit excellent properties such as good solubility and thermal stability, broad absorption especially the absorption peaks of **D-TPA** displayed about 125 to 78 nm red shift for the nature of strong charge transport existing inside the molecules between the conjugated backbone of **TPA** and the acceptor. By connecting different acceptor groups, the band gaps and fluorescence lifetime of small molecules are regulated at the same time. In particular, the effects of different acceptors unit on fluorescence lifetime are researched by instant photo-luminescence spectroscopy. We found that the photo-luminescence lifetimes could be tuned by changing the acceptor units. At length, **D-TPA** displayed the longest photo-luminescence lifetime, 85 ps, which is longer than **R-TPA** and **C-TPA**. The **D-TPA** based on **D** unit exhibits a higher V_{oc} of 0.673 V and PCE of 0.802 %, because of its smaller band-gap, longer exciton lifetime. Although the efficiencies of solar cells are not outstanding, the work we did was already optimized. Unlike many hybrid solar cells with **TPA** as the main structure, we regard it more as the bridging group and study the effect of TiO_2 film morphology on its performance [42-45]. We offer a new idea to improve the performance of hybrid solar cells by increasing the fluorescence lifetime of electron donors. The scalability in tuning the PL lifetimes makes those small molecules promising active layer material for solar cells. It is expected that the photo-luminescence lifetime can be prolonged even further to ensure that excitons get efficient separation with further design and construction such as altering the acceptor units, and the narrow energy gap, small molecules can achieve better optical properties.

AUTHOR CONTRIBUTIONS

S.Q. Liu synthesized the dyes and drafted the manuscript; X. Li fabricated the solar cell; Y. Xie provided the idea; Y.C. Qin guided the experiment and writing process; M.J. Liu conducted the TGA measurement; J.S.Zhao review and edited the paper.

FOUNDING

The work was financially supported by the National Natural Science Foundation of China (51663018, 21667019), the Key Project of Natural Science Foundation of Jiangxi Province (No. 20171ACB20016), the Jiangxi Province Major Academic and Technical Leaders Cultivating Object Program (No. 20172BCB22014), the Science and Technology Department of Jiangxi Province (No. 20181BCB18003 and 20181ACG70025), Natural Science Foundation of Jiangxi Province (20161BBG70043), and Jiangxi Province Education Department of Science and Technology Project (DB201602037, DA201602063).

CONFLICTS OF INTEREST

The authors declare no conflict of interest.

References

1. L. Lu, W. Chen, T. Xu, L. Yu, *Nat. Commun.*, 6 (2015) 1.
2. L. Huo, T. Liu, X. Sun, Y. Cai, A.J. Heeger, Y. Sun, *Adv. Mater.*, 27 (2015) 2938.
3. C. Liu, C. Yi, K. Wang, Y. Yang, R.S. Bhatta, M. Tsige, S. Xiao, X. Gong, *ACS Appl. Mater. Inter.*, 7 (2015) 4928.
4. V. Vohra, K. Kawashima, T. Kakara, T. Koganezawa, I. Osaka, K. Takimiya, H. Murata, *Nat. Photonics*, 9 (2015) 403.
5. Y. Wang, P. Shao, Q. Chen, Y. Li, J. Li, D. He, *J. Appl. Phys.*, 50 (2017)175105.
6. Y. Sun, G.C. Welch, W.L. Leong, C.J. Takacs, G.C. Bazan, A. Heeger, *Nat. Mater.*, 11 (2011) 44.
7. Y. Chen, X. Wan, G. Long, *Accounts Chem. Res.*, 46 (2013) 2645.
8. G. Long, X. Wan, B. Kan, Z. Hu, X. Yang, Y. Zhang, M. Zhang, H. Wu, F. Huang, S. Su, Y. Cao, Y. Chen, *ChemSusChem*, 7 (2014) 2358.
9. Q. Zhang, B. Kan, F. Liu, G. Long, X. Wan, X. Chen, Y. Zuo, W. Ni, H. Zhang, M. Li, Z. Hu, F. Huang, Y. Cao, Z. Liang, M. Zhang, T.P. Russell, Y. Chen, *Nat. Photonics*, 9 (2015) 35.
10. Y. Qin, Y. Cheng, L. Jiang, X. Jin, M. Li, X. Luo, G. Liao, T. Wei, Q. Li, *ACS Sustain. Chem. Eng.*, 3 (2015) 637.
11. H. Y. Abbasi, A. Habib, M. Tanveer, *J. Alloy. Compd.*, 690 (2017) 21.
12. H.W. Cho, W.P. Liao, W.H. Lin, M. Yoshimura, J.J. Wu, *J. Power Sources*, 293 (2015) 246.
13. H. Wang, A.D. Sheikh, Q. Feng, F. Li, Y. Chen, W. Yu, E. Alarousu, C. Ma, M.A.Haque, D. Shi, Z.S. Wang, O.F. Mohammed, O.M. Bakr, T. Wu, *ACS Photonics*, 2 (2015) 849.
14. Q. Xu, T. Song, W. Cui, Y. Liu, W. Xu, S.T. Lee, B. Sun, *ACS Appl. Mater. Inter.*, 7 (2015) 3272.
15. J. Yuan, A. Gallagher, Z. Liu, Y. Sun, W. Ma, *J. Mater. Chem. A*, 3 (2015) 2572.
16. F. Wu, Q. Qiao, B. Bahrami, K. Chen, K. R. Pathak, S. Mabrouk, Y. Tong, X. Li, T. Zhang, R. Jian, *Appl. Surf. Sci.*, 456 (2018) 124.
17. M.N. Shan, S.S. Wang, Z.Q. Bian, J.P. Liu, Y.L. Zhao, *Sol. Energ. Mat. Sol. C.*, 93 (2009) 1613.
18. E.L. Unger, F. Spadavecchia, K. Nonomura, P. Palmgren, G. Cappelletti, A. Hagfeldt, E.M.J. Johansson, G. Boschloo, *ACS Appl. Mater. Inter.*, 4 (2012) 5997.
19. T.M. Clarke, J.R. Durrant, *Chem. Rev.*, 110 (2010) 6736.
20. Y. Lin, Y. Li, X. Zhan, *Chem. Soc. Rev.*, 41 (2012), 4245.
21. H. Bai, Y. Wang, P. Cheng, Y. Li, D. Zhu, X. Zhan, *ACS Appl. Mater. Inter.*, 6 (2014) 8426.
22. M. Cheng, X. Yang, C. Chen, Q. Tan, L. Sun, *J. Mater. Chem. A*, 2 (2014) 10465.
23. S.A. Adonin, L. A. Frolova, M. N. Sokolov, G.V. Shilov, D.V. Korchagin, V.P. Fedin, S. M. Aldoshin, K. J. Stevenson, P.A. Troshin, *Adv. Energy Mater.*, 8 (2017) 1140.
24. J. Min, Y.N. Luponosov, A.N. Solodukhin, N. Kausch-Busies, S.A. Ponomarenko, T. Ameri, C.J. Brabec, *J. Mater. Chem. C*, 2 (2014) 8432.
25. H. Shang, H. Fan, Y. Liu, W. Hu, Li, Y. X. Zhan, *Adv. Mater.*, 23 (2011) 1554.
26. Y. Zhang, H. Tan, M. Xiao, X. Bao, Q. Tao, Y. Wang, Y. Liu, R. Yang, W. Zhu, *Org. Electron.*, 15 (2014) 1173.
27. P. Cheng, X. Zhan, *Chem. Soc. Rev.*, 45 (2016) 2544.
28. H.I. Lu, C.W. Lu, Y.C. Lee, H.W. Lin, L.Y. Lin, F. Lin, J.H. Chang, C.I. Wu, K.T. Wong, *Chem. Mater.*, 26 (2014) 4361.
29. Z. Du, Y. Chen, W. Chen, S. Qiao, S. Wen, Q. Liu, D. Zhu, M. Sun, R. Yang, *Chemistry, an Asian journal*, 9 (2014) 2621.
30. W. Ni, M. Li, B.Kan, Y. Zuo, Q. Zhang, G. Long, H. Feng, X. Wan, Y. Chen, *Org. Electron.*, 15

- (2014) 2285.
31. H.J. Lee, H.C. Leventis, S.A. Haque, T. Torres, M. Grätzel, M.K. Nazeeruddin, *J. Power Sources*, 196 (2011) 596.
 32. H. Cao, W. He, Y. Mao, X. Lin, K. Ishikawa, J.H. Dickerson, W.P. Hess, *J. Power Sources*, 264 (2014) 168.
 33. L.H. Chang, C.K. Hsieh, M.C. Hsiao, J.C. Chiang, P.I. Liu, K.K. Ho, C.C.M. Ma, M.Y. Yen, M.C. Tsai, C.H. Tsai, *J. Power Sources*, 222 (2013) 518.
 34. R. Tang, Z.A. Tan, Y. Li, F. Xi, *Chem. Mater.*, 18 (2006) 1053.
 35. Y. Qin, X. Li, W. Sun, X. Luo, M. Li, X. Tang, X. Jin, Y. Xie, X. Ouyang, Q. Li, *RSC Adv.*, 5 (2015) 2147.
 36. X.J. Yang, M. Wang, J.S. Zhao, C.S. Cui, S.H. Wang, J.F. Liu, *J. Electroanal. Chem.*, 714-715 (2014) 1.
 37. S. Li, G.L. Liu, X.P. Ju, Y. Zhang, J.S. Zhao, *Polymers*, 9 (2017) 173.
 38. K. Usman, S. Ming, X. Liu, X. Li, Z. Gui, Q. Xie, W. Zhang, Y. Wu, H. Q. Wang, J. Fang, *Appl. Nanosci.* 8 (2018) 715
 39. M.S. Kwon, J. Gierschner, J. Seo, S.Y. Park, *J. Mater. Chem. C.*, 2 (2014) 2552.
 40. J. Tang, J.L. Huan, W.J. Wu, J. Li, Z.G. Jin, Y.T. Long, H. Tian, *Energy. Environ. Sci.*, 3 (2010) 1736.
 41. Y. Qin, Y. Cheng, L. Jiang, X. Jin, M. Li, X. Luo, G. Liao, T. Wei, Q. Li, *ACS Sustain. Chem. Eng.*, 3 (2015) 637.
 42. X.L. Liu, L.Q. Kong, H.M. Du, Y. Zhang, J.S. Zhao, Y. Xie, *Org. Electron.*, 64(2019), 223.
 43. E.L. Unger, F. Spadavecchia, K. Nonomura, *Acs Appl. Mater. Inter.*, 4 (2012) 5997.
 44. Y. Qin, S. Liu, H. Gu, W. Dai, X. Luo, *Solar Energy*, 166 (2018) 450.
 45. Z. Xu, M. Wang, J.S. Zhao, C.S. Cui, W.Y. Fan, J.F. Liu, *Electrochim. Acta.*, 125 (2014) 241.